J. COMBIN. MATH. COMBIN. COMPUT. 127b (2025) 8055--8077

Journal of Combinatorial Mathematics
and Combinatorial Computing
www.combinatorialpress.com/jcmcc

Creative and Visual Analysis of Art Design with Computer Image Assisted Systems

Changfu Yang[1], Zhaoting Li[2,✉]

[1] *College of Arts and Design, Ningbo University of Finance & Economics, Ningbo, Zhejiang, 315175, China*
[2] *Department of Film Press and Contents at the Graduate College, Cheongju University, Cheongju-si, Chungcheongbuk-do, 28503, South Korea*

ABSTRACT

Computer image-assisted design, as a product born in the era, provides more inspiration and creativity for art design. Based on the study of the basic theory of color design and the theory of color harmonization, an intelligent color matching model integrating visual aesthetics based on conditional generation adversarial network is proposed. Then a candidate graphic layout generation method based on visual saliency is proposed, which not only considers the visual saliency of each element in the image, but also considers how to generate candidate text regions under the constraints of aesthetic rules. In the visual analysis analysis experiment, under different color transformations, the F-value of the subject's gaze time was 2.548, with significance P=0.051, which is not significant. The F-value of average gaze point is 6.398, significance P=0.002, significant difference is obvious. From this, it can be concluded that the artistic innovation design method proposed in this paper can make the subject's point of interest change with a large difference, and the color that highlights the target object can significantly attract people's attention, which is a feasible artistic innovation design scheme.

Keywords: color matching, graphic layout, conditional generation adversarial network, art design creativity, visual analysis

1. Introduction

Entering the 21st century, the era of information technology has ushered in a phase of rapid development, thanks to the support of computer and Internet technology, human beings have entered the digital era [1-2]. Driven by the rapid development of computers, Internet technology and multimedia technology, human production, lifestyle and way of thinking have undergone obvious changes, and the same art and design has also produced new changes with the development of information science and technology [3-5].

✉ Corresponding author.
E-mail address: lizhaoting1111@163.com (Z. Li).
Received 12 January 2024; Revised 15 March 2024; Accepted 20 November 2024; Published Online 16 April 2025.
DOI: 10.61091/jcmcc127b-440

Nowadays, computer technology and art design combined with the application of the development of faster and faster, relying on computer technology application tools are endless, whether it is Photoshop, AutoCAD, Maya, 3D modeling or virtual reality technology, have brought unprecedented convenience and possibilities for art design [6-8]. Overall, application tools relying on computer technology are based on the basic elements of painting composition, and through subroutines to generate one drawing function after another, designers are able to quickly generate a variety of patterns and combinations, change a variety of color combinations, and preview the design effect through commands [9-11]. Computer technology can be applied not only to graphic art design, but also to three-dimensional art design [12].

Through computer-aided design, designers can realize the visual effects of many traditional visual media. Through computer software, designers can not only realize such as brush, oil painting, watercolor, printmaking and other picture effects, more importantly, can also quickly and easily realize the art characters, gradient effects, light effects and other complex visual effects [13-14]. And not only can these artistic effects be realized alone, art designers can also combine these artistic effects, such as inserting Chinese painting effects in oil paintings, adding simplicity in prints, etc., so that the relevant works of art can achieve the effects that could not be achieved by hand-painted creations in the past [15-16].

The article combines the basic theory of color design and the theory of color harmony to assist the computer to quickly and effectively generate a reasonable and innovative color image scheme. On this basis, the article proposes an intelligent color matching algorithm that integrates visual aesthetics, constructs a visual aesthetic data flow by using eye tracking technology, and constructs an intelligent color matching model that integrates visual aesthetics with an image translation model as the backbone network. Then a deep learning model is proposed to generate a candidate graphic layout, which uses a visual saliency detection network to calculate the visual importance of each part of the input image, and then the diffusion equation is used to calculate the probability map of the text position, while a candidate region generation algorithm is used to obtain a candidate text layout. Finally, the image color matching effect of this paper's method is comprehensively evaluated and visually analyzed by using quantitative evaluation methods and subjective evaluation methods.

2. Method

2.1. Theoretical basis of computer-aided color design

2.1.1. Overview of computer-aided color design. In the background of the computer has become the main tool to assist product design, the importance of color design in product design determines the use of computer-assisted product color design is an inevitable choice. Computer-aided color design is in a variety of computer software systems to assist the color design of creative activities, it is a special design means, with high efficiency, fast, standardized, accurate color synthesis advantages, can achieve rapid conversion of color design, accumulation and reuse, can to a large extent to improve the effect and efficiency of product color design.

2.1.2. Basic Theory of Color Design:

1) Properties of color. Color is light on the object, through the absorption and reflection of color light on the surface of the object, and then act on the visual organs and the formation of color sensation [17]. All the colors that can be perceived by vision can be represented by three attributes: hue, lightness and purity, which are the most basic attributes of color, and people use the three attributes of color to recognize and describe color.

2) Color three-dimensional structure and color sequence system. The International Commission on Illumination's standard chromaticity system is based on 2 sets of basic visual experimental data, using R, G, B the number of three primary colors - the three stimulus values to express the color, and its chromaticity coordinates refers to the relative proportions of each of the three primary colors in $R+G+B$ the total amount. Let the chromaticity coordinates of a color C be r, g, and b then there are:

$$\begin{cases} r = \dfrac{R}{R+G+B} \\ g = \dfrac{G}{R+G+B} \\ b = \dfrac{B}{R+G+B} \\ (C) = r(R) + g(G) + b(B) \end{cases} \tag{1}$$

The value of b can be calculated as long as the values of r and g are known, so the values of r and g can represent 1 color.

The three primary colors can be matched into standard white light and the three stimulus values of standard white light are equal:

$$(W) = 0.33(R) + 0.33(G) + 0.33(B) \tag{2}$$

The CIE chromaticity diagram with a horseshoe shape is thus obtained. The CIE color system is more objective, but has the disadvantage that it is not user-friendly to directly associate with specific colors.

3) Color representation and conversion in computers. The most traditional way to convert the RGB color model to the Menzel HVC color system is:

In the first step, the transition is made through the CEI color space, which is an optically based color standard common to the world, and its color gamut represents the gamut of all visible light.

In the second step, the CIE1931 chromaticity diagram corresponding to nine constant hue and constant chromaticity trajectories with luminance values of 1, 2, ..., 9, respectively, is converted by means of a look-up table, and then linear interpolation is applied to perform the arithmetic to finally complete the conversion work.

Although the color range (color gamut) represented by each color space is different, some simplified conversion methods can meet the general accuracy requirements in the commonly used color range. For example:

1) RGB to HVC conversion method. Let the color value of a color in RGB color space be (r,g,b) and find its color value (h,v,c) in HVC mode by the following procedure:

Assume $m = MAX(r,g,b)$, $n = MIN(r,g,b)$, where $MAX(\cdots\cdots)$ and $MIN(\cdots\cdots)$ are the maximum and minimum values of all the values in the parentheses.

Then:

$$
\begin{aligned}
&v = m \\
&c = \begin{cases} (m-n)/m, m \neq 0 \\ 0, m = 0 \end{cases} \\
&h = \begin{cases} 0, c = 0 \\ 60(g-b)/(m-n), r = m \,\&\, g \geq b \\ 360 + 60(g-b)/(m-n), r = m \,\&\, g < b \\ 120 + 60(b-r)/(m-n), g = m \\ 240 + 60(r-g)/(m-n), b = m \end{cases}
\end{aligned} \tag{3}
$$

2) HVC to RGB conversion algorithm. Let the color value of a color in HVC color space be (h, v, c), find its color value (r, g, b) in RGB color space, the process is as follows:

If $h = 360$, assign h the value 0, i.e. $h = 0$.

Let $i = [h/60] f = [h/60 - i]$, i.e., i be the number by which h is divisible by 60, and f be the remainder by which 60 is divisible.

$$
\begin{aligned}
&p = v * (1-c) \\
&q = v * (1 - c * f) \\
&t = v * (1 - c(1-f))
\end{aligned} \tag{4}
$$

Then:

$$
\begin{cases} When\ i = 0, r = v, g = t, b = p \\ When\ i = 1, r = q, g = v, b = p \\ When\ i = 2, r = p, g = v, b = t \\ When\ i = 3, r = p, g = q, b = v \\ When\ i = 4, r = t, g = p, b = v \\ When\ i = 5, r = v, g = p, b = q \end{cases} \tag{5}
$$

2.1.3. Color Harmony Theory. From the point of view of color balance, the theory of Menzel's color reconciliation of colors with components to represent the interrelationships, the combination of colors will be mixed if it can not become a neutral gray, you can change the purity or area of one of the colors [18], expressed in the formula as:

$$
\frac{Brightness \times purity\ of\ color\ A}{Lightness \times purity\ of\ color\ B} = \frac{Area\ of\ B}{Area\ of\ A} \tag{6}
$$

Accordingly, the balance of the color area becomes the ratio of the product of the luminance figure and the purity figure. Menzel's theory of color harmony states that harmony can be achieved by satisfying the following seven order relationships between colors.

The Monsignor Spencer Color Harmony Theory proposes a quantitative description of color harmony. It is proposed that the interval between the color is not in the mixing area, the combination of a number of color composition is a simple geometric figure, so the color is comfortable, pleasing to the eye and harmony. Meng-Spencer color harmony theory of color hue, luminance and chromaticity, respectively, the interval to do a quantitative definition. For hue, the 100 equal parts of Menzel's hue ring are divided into 8 zones.

Same Color Harmonization Zone: Includes only the zero point of the base color and the interval with a very small distance from the zero point.

Similar Harmonization Zone: Two zones that are around the zero point and the distance from the zero point is between 7 to 12 equal points.

Contrasting Reconciliation Zone: It is the zone that is almost half of the color ring on the opposite side with a distance of more than 28 equidistant points from the zero point.

The first mixing and montage area: located between the similar tonal area and the same color tonal area, that is, on both sides of the zero point and the zero point distance between 0 ~ 7 equidistant points between the left and right two areas.

The second mixed montage area: respectively, in the similar tonal area and contrast between the tonal area, i.e., on both sides of the zero point and the zero point distance between 12 ~ 28 equidistant points between the left and right areas.

Corresponding brightness interval and color interval is also divided into the same five regions.

The same color tone and area: and the base color almost no brightness or color difference between the very small area, the area can be regarded as the same color with the base color.

The first mixing zone: the specified degree of difference is about less than 0.5, the color difference is about less than 3 between the region. The difference between the two colors in the area is too small to form a clear boundary between the color blocks.

Similar to the reconciliation zone: is the difference between the brightness of the colors in the 0.5 ~ 1.5, color difference between 3 ~ 5 region.

The second mixed montage area: is the brightness difference between 1.5~2.5, color difference between 5~7 area.

Contrast Harmonization Zone: It is the area where the luminance difference is between 2.5~10 and the color difference is more than 7.

Glare is the area where the difference in brightness between two colors is greater than 10, and the reconciliation is lost because of flare.

The aesthetics formula therein is based on the aesthetics formula for evaluating formal beauty for the comprehensive evaluation of the color-matching problem: $M = O/C$ where, M is the aesthetics, O is the order factor, and C is the complexity factor.

The Mon-Spencer theory experimentally suggests that the order factor O has different values in the evaluation of whether or not chromaticity is involved in color matching, i.e.

$$o = \begin{cases} \sum o_s & \text{(in case of colorless composition only)} \\ \sum o_h + o_v + \sigma_\varepsilon & \text{(when including color)} \end{cases} \tag{7}$$

where O_g is the order factor when there is only a combination of gray without color. O_h, O_v, O_c are the values of the order factors when there is colored participation in color matching, respectively, only the color phase difference, brightness difference or color difference determines the value of each order factor, the value depends on the above color between the attributes of the division of the interval relationship, corresponding to the value of the order factors of different values in the calculation of the no-color can be regarded as the same as the color with any colored phase.

Complexity factor C is composed of:

$$C = C_m + C_n + C_v + C_c \tag{8}$$

where, C_m is the total number of colors in the color scheme, C_h is the number of color pairs with chromatic difference in all possible two-by-two combinations, C_v is the number of color pairs with brightness difference in all possible two-by-two combinations, and the number of color pairs with chromaticity difference in all possible two-by-two combinations. The beauty value M is calculated by the formula, and it is generally believed that $M = 0.5$ when monochromatic, so $M > 0.5$ when the color matching is beautiful, and vice versa is not beautiful.

In addition, different colors together, the proportion of area between the color block will also affect the design effect. Meng - Spencer color harmony theory, two colors to reach a coordinated proportion of the area to follow the “moment of balance principle”. “Moment”, i.e. its scalar moment is defined as:

$$M = A \cdot \|P - P_0\| \tag{9}$$

where A is the area, P is the point P corresponding to the two colors in the $C-V$ plane, P_0 is a reference color, and the distance is defined as:

$$\|P - P_0\| = \sqrt{w_c \cdot (C - C_0)^2 + (V - V_0)^2} \tag{10}$$

2.2. *Design of color matching algorithms incorporating visual aesthetics*

2.2.1. Visual aesthetics. Since the human eye is always attracted to more visually appealing objects, the quantification of visual aesthetics using eye movement behavioral measures is an important technical tool in this field. In the process of quantifying visual aesthetics using eye movement behavioral measures, the three most important eye movement behavioral indicators are average gaze time, average number of gaze points, and first gaze time, which reflect the visual comfort, visual attractiveness, and visual impact of the test image or video, respectively [19]. Taking the average gaze time as an example, its calculation formula in the eye tracking experiment is shown in equation (11).

$$T = \frac{\sum_{i=1}^{n} T(AOI)}{n} \tag{11}$$

Eq:

n - number of test images or videos.

$T(AOI)$ - test time for delineating the region of interest in the eye movement experiment.

In visual search, targets with visual aesthetic appeal usually receive more gazes, and the corresponding eye movement behavioral metrics include average gaze time, average number of gaze points, and first gaze time.

Using eye movement behavior indicators to construct visual aesthetics data flow, the above three eye movement behavior indicators are normalized before processing, in which the average gaze time and the average number of gaze points are positively correlated with the degree of visual aesthetics favoritism, taking the average gaze time as an example, and the processing method is defined as follows:

$$h' = \frac{h - h\_\min}{h\_\max - h\_\min} \tag{12}$$

Eq:

h - the current data to be processed before normalization.

$h\_\min$, $h\_\max$ - the minimum and maximum values of the average gaze time, respectively.

The first gaze time measure is negatively correlated with visual aesthetics favoritism in the interaction task, which is processed as defined below:

$$j = 1 - \frac{j - j\_\min}{j\_\max - j\_\min} \tag{13}$$

Eq:

j - the current data to be processed before normalization.

$j\_\min$, $j\_\max$ - the minimum and maximum values of the first gaze time, respectively.

The visual aesthetic parameter W is shown in equation (14):

$$W = (\alpha h' + \beta i' + \gamma j') \times 10 \tag{14}$$

Eq:

W - the visual aesthetic parameter for fusing three different eye movement behavior data, taking values between $[0,10]$.

α , β , γ - weights of three different eye movement behavior data.

Where the three weights are set differently according to different visual tasks, $\alpha = \beta = \gamma = 1/3$ is used in this chapter to calculate the visual aesthetic score W .

2.2.2. Image translation model. The Image Translation Model (Pix2Pix) is a manifestation of Conditional Generative Adversarial Networks in the image translation task. The image translation model is a conditional generative adversarial network with U-Net and Markov discriminator (GAN) as generator and discriminator, respectively, whose generator input is a real sample image x and output is a generated image $G(x)$. Since the discriminator needs to determine the authenticity of the output image of the generator, the input of the discriminator is a pair of images composed of the generated image $G(x)$ and the real image. The network model diagram of Pix2Pix is shown in Figure 1.

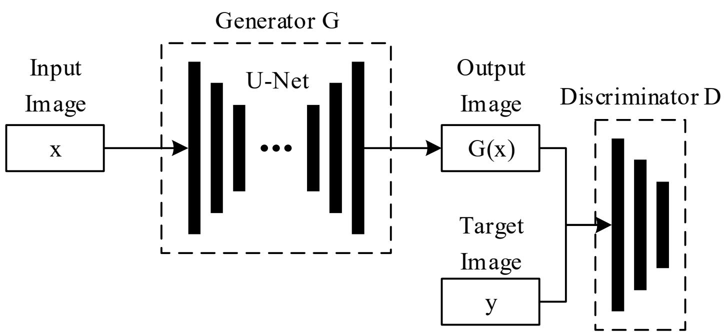

Fig. 1. Network structure of Pix2Pix

In addition, the Pix2Pix network model introduces $L_1 Loss$ to judge the image globally on the basis of CGAN, as shown in equation (15).

$$G^* = \arg\min_G \max_D L_{cGAN}(G,D) + \lambda L_{L_1}(G) \tag{15}$$

Eqs:

G , D - represent generator and discriminator respectively.

$L_{L_1}(G)$, λ - represent the weights of $L_1 Loss$ & $L_1 Loss$ respectively.

Where $L_1 Loss$ is defined as defined below:

$$L_{L_1}(G) = E_{x,y,z}\left[\left\| y - G(x,z) \right\|_1\right] \tag{16}$$

Eq:

G - generator.

x , y , z - denote the real sample, conditional probability, and random noise, respectively.

The loss function of Pix2Pix is shown in equation (17):

$$\begin{aligned} L(G_{\min}, D_{\max}) &= E_{x\sim p_{data}(x)}\left[\log D(x \mid y)\right] \\ &+ E_{z\sim p_z(z)}\left[\log(1 - D(G(z \mid y)))\right] + \lambda L_{L_1}(G) \end{aligned} \tag{17}$$

2.2.3. Intelligent color matching model incorporating visual aesthetics. A palette visual aesthetic evaluation model is constructed using the visual aesthetic parameters with the primary color palette of the corresponding image.The evaluation model is used to score the input palette and subsequently optimize the loss function of the Pix2Pix backbone network using this scoring value. The evaluation model in this chapter uses the SE-Inception V3 network model, which compresses the image features through global average pooling and scores the probability distribution of the image aesthetic quality scores, and uses the true visual aesthetic parameters of the palette as the labels of the corresponding palette to train the scoring model [20]. The palette visual aesthetic evaluation model is shown in Figure 2.

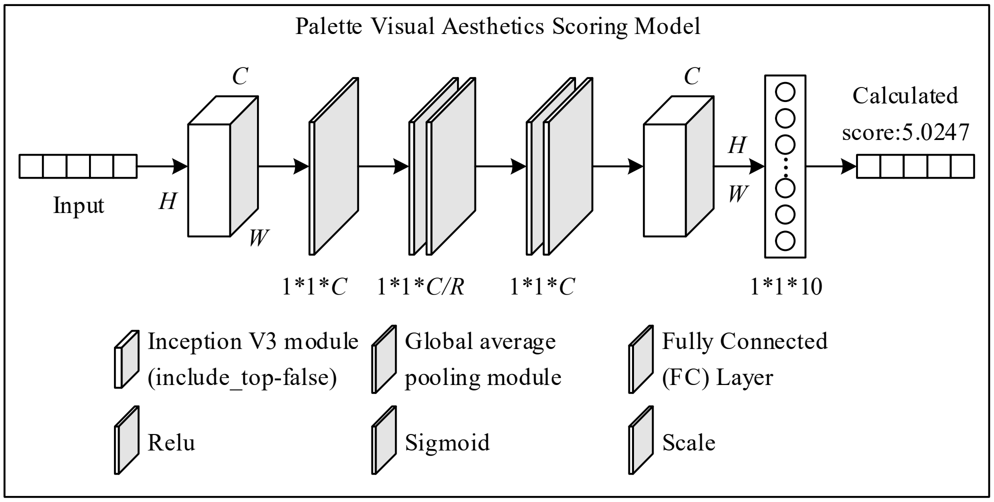

Fig. 2. Palettes visual aesthetic scoring model

The loss function of the backbone network Pix2Pix is updated using the aesthetic scores of the color palette, and the aesthetic loss function $S(G)$ and the total loss function of the intelligent color matching algorithm incorporating visual aesthetics established in this chapter are shown in Eq. (18) and Eq. (19), respectively:

$$S(G) = 10 - Score \tag{18}$$

$$\begin{aligned} L(G_{\min}, D_{\max}) &= E_{x \sim p_{data(x)}}[\log D(x \mid y)] \\ &+ E_{z \sim p_i(z)}[\log(1 - D(G(z \mid y)))] + \lambda L_{L_1}(G) + \gamma S(G) \end{aligned} \tag{19}$$

where: $10 - Score$ - denotes the score of the visual aesthetic scoring model of the color palette and the full score of the aesthetic evaluation, respectively.

γ - the weight of $S(G)$.

The framework of the intelligent color matching algorithm incorporating visual aesthetics is shown in Fig. 3.

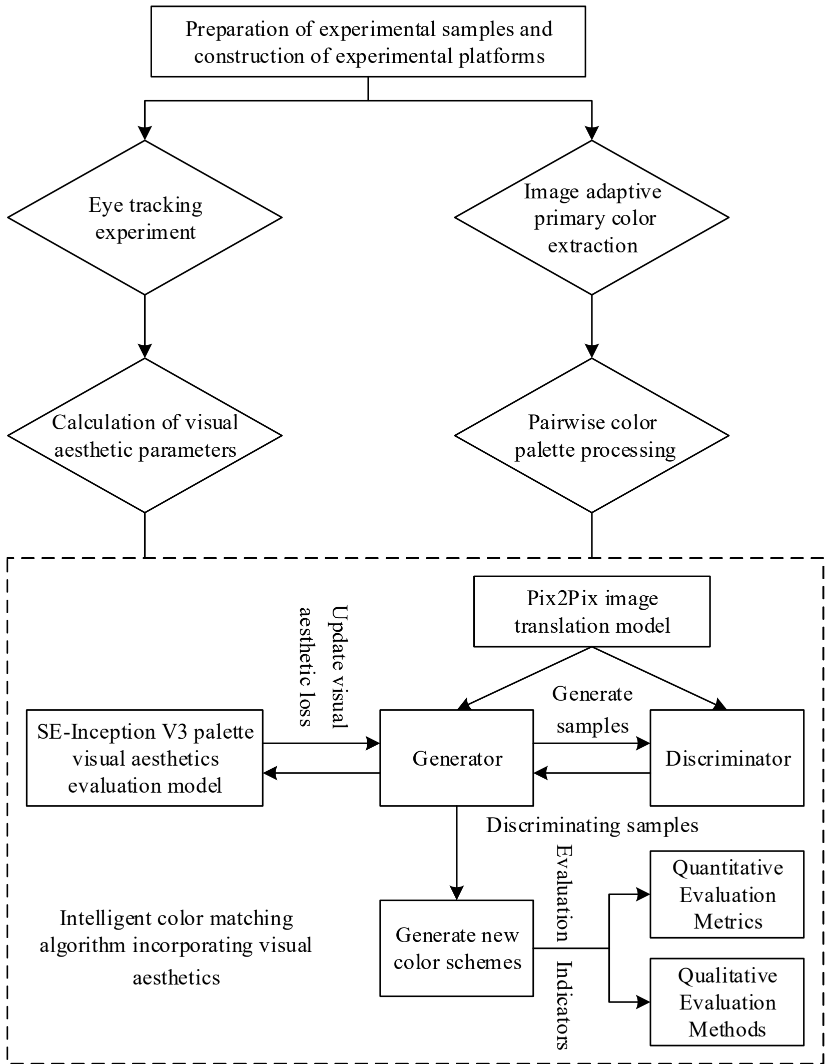

Fig. 3. Framework of intelligent color matching methods that incorporates visual aesthetics

2.3. Candidate graphic layout generation based on visual saliency

Candidate Graphic Layout Generation and Scoring of Graphic Layouts Based on Aesthetic Evaluation. This section focuses on candidate graphic layout generation, where the goal of this phase is to generate some potentially harmonious text layouts on natural images, i.e., given a natural image M_i and a piece of text T_i, output a series of candidate text boxes $M_{o_{set}} = \{M_{o_1}, M_{o_2}, \ldots, M_{o_k}\}$ that differ in position T_p and size T_s.

Unlike some existing graphic design layout methods in the past, which generally require raw fine-grained data, such as the categories of images and the attributes of design elements, the model proposed in this chapter takes a natural image in the form of a bitmap as an input, and does not require finely labeled graphic design data. Candidate graphic layout generation based on visual saliency consists of 2 main components:

1) Visual saliency detection network: the input of this network is the natural image M_i and the output is the corresponding visual saliency map S_M.

2) Text region suggestion algorithm: this algorithm consists of 2 sub-algorithms. The first one is a diffusion equation, the input is a visual saliency map S_M, and the output is a text location probability map PD_M. The second one is a candidate region generation algorithm, the input is a text location

probability map PD_M, and the output is a series of sets of candidate text regions with different locations and sizes $M_{o_{set}} = \left\{M_{o_1}, M_{o_2}, \ldots, M_{o_k}\right\}$.

2.3.1. Visual saliency detection network. Visual saliency detection is the calculation of the visual importance of different elements in a natural image or graphic design. Most of the previous research work is on visual saliency detection of natural images, while less work has been done on visual saliency detection of graphic designs. Although the input background image is a natural image, the generated graphic layout results in a graphic design, so the elements of the background image need to be considered as graphic design elements in the visual saliency detection stage. The difference between the two is that the salient regions of natural images are more concentrated and the exploration of natural image features has been more mature in a large number of past studies. The visual saliency of graphic design, on the other hand, not only depends on the image context, but also relates to higher-level design factors, such as the semantic categories of the elements and the relationships between the elements, etc. In graphic design works, people will tend to treat a design element as a whole, i.e., to give the whole design element a similar visual significance, and there are relevant explanations for this phenomenon in Gestalt theory. In this section, an end-to-end deep learning model is built to predict the visual salience of background images.

The encoder of this network is similar to the Residual Network (ResNet), which uses basic Res Blocks to obtain feature maps at different resolutions. The part that connects the encoder to the decoder is a three-layer convolution consisting of 512 3×3 dilated convolution kernels with a dilation rate of 2. Such connected layers help the network to better capture the global information of the image. The decoder and encoder network structures are basically symmetric, and the input to the convolutional layer at each stage is the connection between the feature map up-sampled at the previous stage and the feature map at the corresponding stage of the encoder. The initial visual saliency map output from the decoder is still fuzzy and noisy, and needs to be fed into the refinement module (RRM) to further improve the accuracy. RRM is a residual learning structure, and each convolutional layer consists of 64 3×3 convolutional kernels, with maximum pooling used for downsampling, and bilinear interpolation used for up-sampling, and the RRM module further refines the prediction of the saliency map by learning the residuals of the predicted saliency map and the real saliency map, adding the residuals to the predicted saliency map. The RRM module further refines the predicted saliency map by learning the residuals between the predicted saliency map and the real saliency map, and the output is the final visual saliency map after adding the residuals to the initial visual saliency map. The structure of the visual saliency detection network is shown in Figure 4.

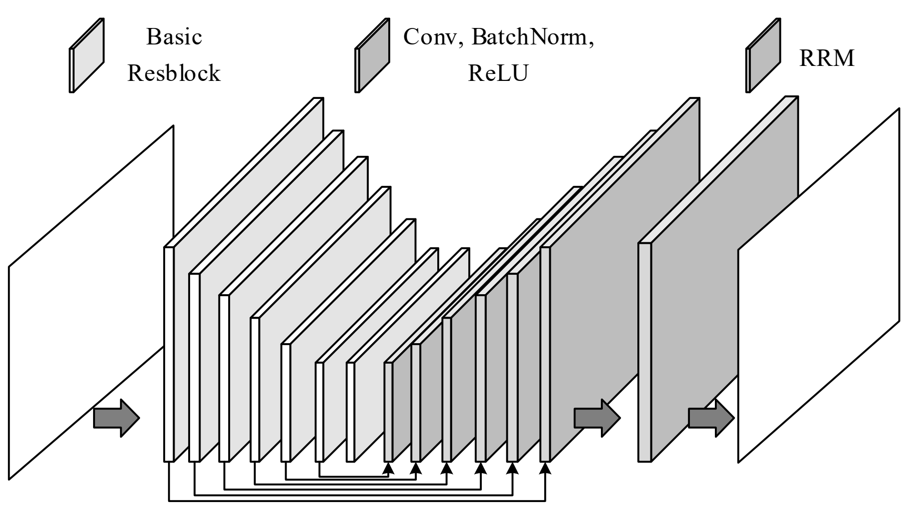

Fig. 4. Visual significance detection network structure

The goal of the original BASNet model is to detect and segment salient objects, but the goal of this section is to compute visual saliency maps at the pixel level, i.e., each pixel has a saliency value in the real-number range of $[0,1]$. Therefore, the loss function for training is defined as the hybrid loss function of Equation (20):

$$L(\Theta) = L_{BCE}(\Theta) + L_{SSIM}(\Theta) \tag{20}$$

where $L_{BCE}(\Theta)$ represents the BCEWith Logits loss function, $L_{SSIM}(\Theta)$ represents the SSIM loss function, and Θ represents the parameters of the visual saliency detection network.

Given a real visual saliency map $G_{M_p} \in [0,1]$, where $p = 1, \ldots, N$ represents each pixel point, the BCEWith Logits loss function is defined as:

$$L_{BCE}(\Theta) = -\frac{1}{N}\sum_{p=1}^{N}\left(G_{M_p}\log S_{M_p} + \left(1 - G_{M_p}\right)\log\left(1 - S_{M_p}\right)\right) \tag{21}$$

where S_{M_p} denotes the visual saliency map predicted by the network.

Assuming that $x = \{x_p \mid p = 1,2,\ldots,N\}$ and $y = \{y_p \mid p = 1,2,\ldots,N\}$ denote the two image regions extracted from saliency maps G_{M_p} and S_{M_p}, μ_x, μ_y and σ_x^2, σ_y^2 denote the mean and variance of x and y, respectively, and σ_{xy} is their covariance, the SSIM loss function can be defined as:

$$L_S(\Theta) = 1 - \frac{\left(2\mu_x\mu_y + C_1\right)\left(2\sigma_{xy} + C_2\right)}{\left(\mu_x^2 + \mu_y^2 + C_1\right)\left(\sigma_x^2 + \sigma_y^2 + C_2\right)} \tag{22}$$

where $C_1 = 0.01^2$, $C_2 = 0.03^2$ are constants set for the training of this network.

2.3.2. Candidate Layout Area Generation:

1) Diffusion Equation. In the past research work, the diffusion equation is widely used in the scenarios of image denoising, image edge extraction, image scale space analysis, etc. The classical Gaussian filter will filter the image edge texture and other information together, making the image too smooth and losing the structural information. The classical Gaussian filter will filter the image edge texture and other information together, making the image too smooth and losing the structural information, etc. The anisotropic diffusion equation can adaptively adjust the diffusion coefficients according to the different local features of the image, which can maintain the edge details between the image elements while making the pixels within the region tend to be smooth. Different from the existing work, guided by the aesthetic rules, this section applies the diffusion equation to calculate the text position probability map, which is defined as follows:

$$\begin{cases} PD_{M+1} = PD_M + \lambda\left(dX + dY\right) \\ dX = c_X \nabla_X\left(PD_M\right), dY = c_Y \nabla_Y\left(PD_M\right) \end{cases} \tag{23}$$

where ∇_X and ∇_Y denote the gradient of the pixel in the horizontal and vertical directions, respectively, and c_X and c_Y denote the diffusion coefficient in both directions, respectively.

2) Candidate region generation algorithm. Section proposes a candidate text region generation algorithm that, unlike past work that utilized raw image features, this algorithm utilizes a text location probability map PD_M. The text location probability map can visually represent the probability of a candidate text region appearing at the corresponding location. Therefore, the greater the probability of the region, the more candidate text boxes should be generated, so that the probability of the appearance of the optimal graphic layout visual effect is also greater. Assuming that the aspect ratio of

the text area is $Ratio_T$, first, select the regions with higher probability in the text position probability map PD_M, calculate the maximum probability value position of each region (here "probability value" is defined as the sum of probability values in the rectangular region), as the initial position of the text area, the coordinates of the upper left corner of the region R_p are (x_1, y_1), and the coordinates of the lower right corner are (x_2, y_2). Then, based on the probability value of each initial candidate text area R_p, the initial text area is offset to generate a new candidate text box, the generation method is as follows:

$$\left\{\left(x_{new_1}, y_{new_1}\right) \mid x_1 - \Delta x \le x_{new_1} \le x_1 + \Delta x, y_1 - \Delta y \le y_{new_1} \le y_1 + \Delta y\right\} \tag{24}$$

where $\left(x_{new_1}, y_{new_1}\right)$ is the coordinate of the upper left corner of the newly generated candidate text region, $\Delta x = \delta\left|x_2 - x_1\right|$, $\Delta y = Ratio_T \Delta x$ denote the offset range of the text box position, and $\delta \propto \sum_{i=1}^{|x_2-x_1|}\sum_{j=1}^{|y_2-y_1|} R_p(i,j)$ denotes the offset coefficient. If the probability value of the initial text region R_p is larger, the offset range Δx is also larger, i.e., more candidate text boxes are generated. The size of the initial text area R_p can have various values while keeping the aspect ratio as $Ratio_T$.

3. Results and discussion

3.1. Analysis of the aesthetics of color matching integrating visual aesthetics

3.1.1. Subjective aesthetic rating research. Based on Monsignor Spencer's Color Harmony Theory, the five color schemes with the highest and lowest quantitative aesthetics before and after the introduction of the junction edge weights were calculated respectively, and a total of 12 color schemes were combined. The 12 art design color schemes were used as research samples to carry out subjective aesthetic rating research. Through the distribution of network questionnaires on 85 subjects to carry out color subjective aesthetic rating research, including 30 men, 55 women, aged 18 to 25 years old. The research used Likert psychometric scales, which are commonly used to measure the respondents' views and attitudes towards a certain product or service, such as like, dislike, agree, disagree and so on. Common Likert scales have 5, 7 and 9 levels, although two more levels can refine the respondents' attitudes, but it will cause the respondents to have difficulty in choosing between the adjacent levels, thus causing the psychological burden of the respondents. Therefore, this paper adopts a 5-level scale with ratings from 1 to 5, indicating a sequential increase from very unattractive to very beautiful levels.

3.1.2. Analysis of Research Results. The correlation test between the color matching beauty values quantified based on Monsignor Spencer's color reconciliation theory and the subjective aesthetic scores before and after the introduction of the junction edge weights was conducted, and the correlation test (before the introduction of the junction edge weights) and the correlation test (after the introduction of the junction edge weights) are shown in Table 1 and Table 2. From the data in the tables, it can be seen that the Pearson correlation coefficients before and after the introduction of the junction edge weights are 0.095 (p=0.781) and 0.315 (p=0.388), respectively, with the p-values of all of them being greater than 0.05. In Pearson correlation analysis, it is usually necessary to have a $p \leqslant 0.05$ in order to consider that there is a significant correlation between the two sets of data, and the opposite is considered to be an insignificant degree of correlation or even no correlation between the two data. Correlation. It can be seen that before and after the introduction of the junction edge weights, there is no correlation between the quantitative values of color matching aesthetics based on Monsignor Spencer's theory of color harmony and the subjective aesthetic scores. However, by comparing the p-values and correlation coefficients before and after the introduction of the junction edge weights, it can be seen that the introduction of the junction edge weights has certain rationality in the color matching beauty metrics.

Table 1. Correlation test (before the boundary of the boundary)

		Subjective (1)
Objective (1)	Pearson correlation	0.095
	Sig.2	0.781
	Case number	10

Table 2. Correlation test (after the boundary of the boundary)

		Subjective (2)
Objective (2)	Pearson correlation	0.315
	Sig.2	0.388
	Case number	10

In summary, the application of Monspencer's color reconciliation theory in color matching beauty metrics before and after the introduction of junction edge weights largely fails to satisfy people's subjective aesthetic needs, but the introduction of junction edge weights can optimize the application of Monspencer's color reconciliation theory in color matching beauty metrics to a certain extent.

3.1.3. Monsignor Spencer Color Harmony Theory Order Factor Value Correction. Through the analysis of the relationship between the matching of color selection can be seen, the vast majority of college students tend to be in the choice of approximate color matching, such as, hue difference between 0~10, color difference between 0~2.4, brightness difference between 0~2. Through the comparison with the order factor value can be found in the chromaticity difference between 0~7 order factor value is 0, brightness difference between 0~0.5 order factor value is negative, saturation difference between 0~3 order factor value is 0, this trend and college students in the color collocation preference does not match, so this paper on the 53 college students color selection collocation relationship analysis, color collocation relationship analysis as shown in Figure 5. The ratio of the number of color matching samples of a certain color dimension in a certain difference interval to the total number of matching samples is taken as the order factor value of the difference of the color dimension in the interval. The corrected order factor value is shown in Figure 6.

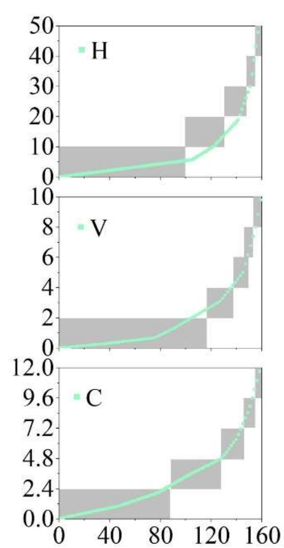

Fig. 5. Color matching analysis

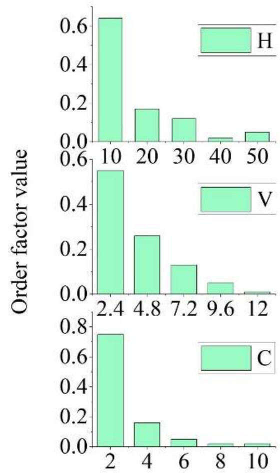

Fig. 6. Corrected order factor

Based on Monspencer's color reconciliation theory and Birkhoff's beauty evaluation model the beauty of image color matching is quantified by correcting the order factor values on the basis of introducing junction edge weights. The beauty quantification by correcting the order factor values is shown in Table 3. The color schemes ranked from 1 to 5 are the five schemes with the highest beauty values, and the color schemes ranked from 6 to 10 are the five schemes with the lowest beauty values.

Table 3. To measure the beauty of order factors

Ranking	Color scheme	Color number	H, V, C	Order factor O	Complexity factor C	American value M	M total
No.1	A	1	A(9.59, 6.79, 6.57)	O_{AB}(0.62, 0.53, 0.66)	C_{AB}:1	M_{AB}:1.87	1.82
			B(9.55, 6.85, 6.49)	O_{AC}(0.61, 0.52, 0.72)	C_{AC}:1	M_{AC}:1.91	
			C(9.32, 6.89, 6.54)	O_{BC}(0.63, 0.44, 0.84)	C_{BC}:1	M_{BC}:1.89	
No.2	B	2	A(10.55, 4.72, 7.11)	O_{AB}(0.54, 0.53, 0.65)	C_{AB}:1	M_{AB}:0.37	1.12
			B(10.53, 4.92, 7.35)	O_{AC}(0.65, 0.5, 0.7)	C_{AC}:6	M_{AC}:1.85	
			C(10.45, 4.73, 7.19)	O_{BC}(0.63, 0.53, 0.75)	C_{BC}:1	M_{BC}:0.4	
No.3	C	2	A(11.47, 3.02, 7.12)	O_{AB}(0.6, 0.42, 0.79)	C_{AB}:6	M_{AB}:0.33	1.12
			B(10.71, 4.25, 5.86)	O_{AC}(0.62, 0.52, 0.75)	C_{AC}:6	M_{AC}:1.85	
			C(11.38, 2.91, 7.31)	O_{BC}(0.55, 0.43, 0.75)	C_{BC}:6	M_{BC}:0.41	
No.4	D	2	A(27.58, -1.63, 8.07)	O_{AB}(0.63, 0.53, 0.73)	C_{AB}:6	M_{AB}:0.29	1.05
			B(28.9, -1.17, 7.87)	O_{AC}(0.68, 0.55, 0.71)	C_{AC}:6	M_{AC}:1.87	
			C(27.58, -1.78, 8.04)	O_{BC}(0.55, 0.48, 0.7)	C_{BC}:6	M_{BC}:0.37	
No.5	E	3	A(8.55, 11.9, 5.72)	O_{AB}(0.65, 0.09, 0.77)	C_{AB}:6	M_{AB}:0.23	0.21
			B(3.58, 2.55, 3.9)	O_{AC}(0.63, 0.64, 0.7)	C_{AC}:6	M_{AC}:0.17	
			C(8.55, 12.06, 5.98)	O_{BC}(0.6, 0.02, 0.72)	C_{BC}:6	M_{BC}:0.14	
No.6	F	3	A(9.87, 5.58, 7.5)	O_{AB}(0.2, 0.27, 0.74)	C_{AB}:6	M_{AB}:0.33	0.23
			B(-6.48, 2.32, 8.29)	O_{AC}(0.1, 0.06, 0.71)	C_{AC}:6	M_{AC}:0.08	
			C(30.81, -2.56, 8.4)	O_{BC}(0.02, 0.1, 0.67)	C_{BC}:6	M_{BC}:0.22	
No.7	G	3	A(11.54, 8.56, 6.4)	O_{AB}(0.59, 0.42, 0.75)	C_{AB}:6	M_{AB}:0.17	0.19
			B(13.05, 6.92, 4.59)	O_{AC}(0, 0.08, 0.14)	C_{AC}:6	M_{AC}:0.05	
			C(39.24, 0.84, 4.03)	O_{BC}(0.09, 0.16, 0.8)	C_{BC}:6	M_{BC}:0.26	
No.8	H	3	A(31.23, -1.76, 3)	O_{AB}(0.23, 0.55, -0.02)	C_{AB}:6	M_{AB}:0.12	0.19
			B(11.15, -0.05, 8.81)	O_{AC}(0.05, 0.28, 0.07)	C_{AC}:6	M_{AC}:0.11	
			C(-6.41, 2.05, 7.27)	O_{BC}(0.25, 0.47, 0.69)	C_{BC}:6	M_{BC}:0.21	
No.9	I	3	A(29.61, 5.49, 3.7)	O_{AB}(0.16, 0.25, 0.16)	C_{AB}:6	M_{AB}:0.05	0.18
			B(9.9, 9.76, 6.62)	O_{AC}(0.67, 0.12, 0.12)	C_{AC}:6	M_{AC}:0.26	
			C(22.22, -0.56, 7.89)	O_{BC}(0.2, 0.03, 0.71)	C_{BC}:6	M_{BC}:0	
No.10	J	3	A(4.01, 9.58, 5.39)	O_{AB}(0.11, 0.01, 0.16)	C_{AB}:6	M_{AB}:1.87	0.16
			B(32.56, -0.16, 2.13)	O_{AC}(0.62, 0.27, 0.2)	C_{AC}:6	M_{AC}:1.91	
			C(12.31, 6.14, 7.77)	O_{BC}(0.12, 0.13, 0.05)	C_{BC}:6	M_{BC}:1.89	

The subjective aesthetic score research was repeated with the 10 color schemes as the research sample, and the correlation test between the quantitative beauty value and the subjective aesthetic score was conducted, and the correlation test (after correcting the value of the order factor) is shown in Table 4. The correlation coefficient is 0.641 ($p=0.045<0.05$), which is a highly positive correlation, and it can be seen that correcting the values of the order factors in Monsignor Spencer's theory of color mixing can optimize the use of color matching algorithms integrating visual aesthetics in the quantification of the aesthetic value of color matching to a greater extent.

Table 4. Correlation test (after the order factor value)

		Subjectivity
Objectivity	Pearson Correlation	0.641
	Sig.2	0.045
	The Sum Of Squares And The Cross Product	2.284
	Covariance	0.263
	Case Number	10

3.2. Experiments on the effect of graphic layout generation

3.2.1. Experimental setup. The purpose of the experimental users is, to verify the validity of the methodology proposed in this chapter under different criteria and different topics. With this aim in mind, two tasks were designed:

Task 1: "Criteria control" For each participant, 10 control groups were randomly selected from all the materials. In each control group, participants were presented with 4 graphic presentations. The different methods were presented in terms of text placement, text readability, global color coordination, font emotional consistency, and overall rating score as shown in Figure 7. The participants then ranked the 4 layouts according to the criteria given.

Task 2: "Theme Control" In this task, participants were asked to view all the layouts for a particular theme and to give an overall rating for the generation method.

The scale ranges from 1 to 9, with 5 being the middle score. The higher the score, the more satisfied the participant is with the results. In this section, the questionnaire was administered to 20 individuals ranging in age from 18 to 30 years old. Between every two control groups, there was a short break so as to ensure that the participants were not tired. Similarly, the distribution of the graphs produced in different ways was displayed randomly so as to prevent participants from being biased in their scoring. For each participant, it took about 1 hour to complete the study. From the results of the experiment, it can be concluded that the participants gave full consideration to factors such as text proportion and variability before giving an overall rating. The scores of the results achieved by the method proposed in this chapter are close to the scores of the manually designed covers. This indicates that the method proposed in this paper is more practical compared to previous work.

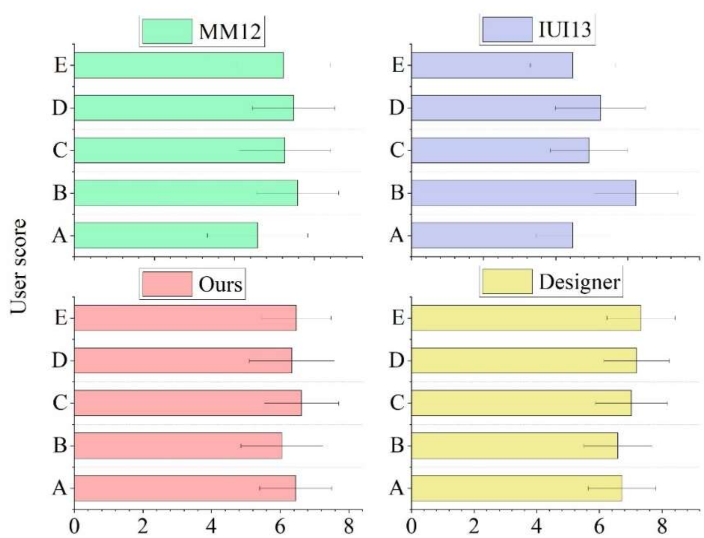

Fig. 7. Scores of different methods

3.2.2. Quantitative assessment. By implementing a user study, this chapter collected ratings and compared the approach proposed in this chapter with previous work and the final performance of the designers. The validity of the theme-based template approach proposed in this paper is confirmed. The following is a summary of the two quantitative analyses and the feedback for the participating users. The quantitative user study led to the following experimental conclusions:

In this section of the experiment, a quantitative user study was conducted to compare and contrast the methods for 8 common themes with an overall evaluation. The overall rating scores of the different methods for the 8 common themes are shown in Fig. 8. The partially reproduced scores of the MM'12 method are higher than those of the IUI'12 method, proving that people prefer conservative chunk-based layouts to cluttered ones. The method proposed in this section scores higher than the first two because, for each topic, this section uses spatial layout templates and topic-based styles, which help to generate more eye-pleasing graphical presentations. It is worth noting that the overall ratings for each theme were generally higher than those of the control group in the final study. The reason for this was discovered by collecting user feedback from the participants; people are usually impressed by the highest results and thus base their overall rating on the highest score in the theme.

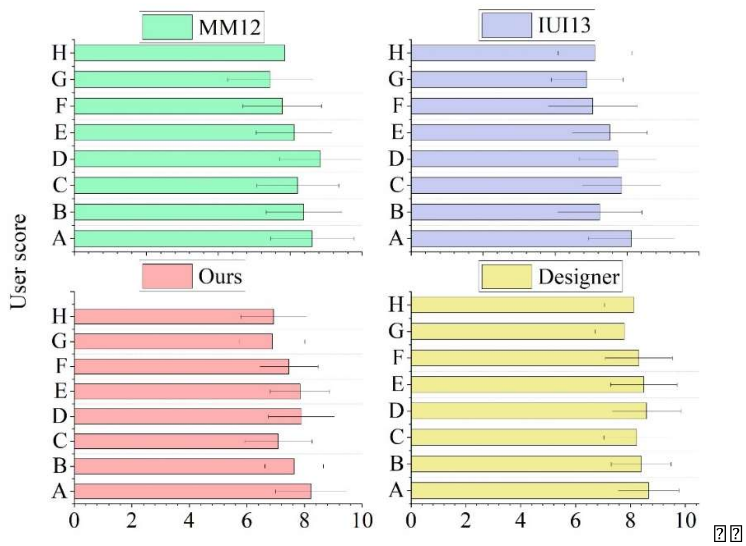

Fig. 8. Different methods are scored in eight common topics

3.3. Visual analysis of artistic design ideas

When evaluating the attention effect, most of them use two indexes, the average gaze time and the number of gaze points, the longer the gaze time, the greater the degree of attraction of the subject to the target area, and the more gaze points, the greater the scope of attention of the subject to the target area, the combination of which responds to the overall attention effect. This paper mainly studies the visual attention effect of images, so after collecting and organizing the experimental data, it mainly focuses on the average gaze time and gaze points in the results of the two data to carry out one-way ANOVA respectively.

3.3.1. Color factor significance analysis. This group of experiments examines the effect of color change on the overall visual attention index of plane images. A more colorful subject image is chosen, and the overall structure and image content are more complex, so as to attract the attention of the subjects more, and it is easy to eliminate the interference between other image elements, so that the experimental results are more scientific. On this basis, two kinds of changes were made to the color tone until black and white tone, and the average gaze time and average gaze point of the subjects under different color tones were recorded respectively. According to the statistical results, the average gaze time of the subjects under the bright color tone was the largest, which was 236, and the average gaze point was also the largest, which was 26. The attention time under black and white hues was the next largest at 215, and the attention time under grayscale hues was the least at 208, and there was little difference between grayscale and black and white hues in terms of the mean attention points. The variance of the mean attention time is large, which indicates that there is a significant difference in the attention time of different subjects to the image, while the variance of the mean attention point is relatively small, which indicates that there is not much difference in the attention range of different subjects. The statistics of attention time and attention point of different color elements are shown in Table 5.

Table 5. Different color elements watch time and watch point statistics

	Average fixation(ms)	SD	Fixation count(n)	SD
Bright tone	236	41.6	26	4.6
Gray tone	208	45.9	24	6.3
Black and white tone	215	52.8	23	5.5

Before performing one-way ANOVA on the color elements, a variance chi-square test was first performed. The variance chi-square test for color elements is shown in Table 6. According to the results of the chi-square test, the probability of chi-square of the variance of gaze time and gaze point is 0.374 and 0.284 respectively, which are greater than 0.05, indicating that there is no significant difference in the variance of each group at the level of α =0.05, i.e., it is considered to be chi-square, and significance analyses can be conducted.

Table 6. Color factor variance homogeneity test

	Levene statistic	Df1	Df2	Significance
Fixation time(ms)	1.041	2	85	0.374
Fixation point(n)	1.267	2	85	0.284

The results of one-way ANOVA for color elements are shown in Table 7. As can be seen from the results of the analysis of the significance of the color elements of the table, the F-value of the subject's gaze time under different color transformations is 2.548, and the significance P=0.051 is close to 0.05, indicating that the significance is not significant. The F-value for average gaze point was 6.398, with significance P=0.002<0.05, indicating a significant difference. This shows that the change of color can make the subject's point of interest change in a large difference, so the method in this paper is a feasible image design scheme.

Table 7. The analysis of the variance analysis of color factors

	Mean square	F value	Significance
Fixation time(ms)	6514.6	2.548	0.051
Fixation point(n)	196.5	6.398	0.002

Due to the significant differences in the changes of color elements at the gaze points, further multiple comparisons of the gaze points were performed to analyze the significance of the differences between the individual color differences. The comparison between the groups of significance analysis of the gaze points is shown in Table 8. According to the results of the table, it can be seen from the level of significance, the first and second category of colors of the visual attention point index comparison of significance P = 0.264> 0.05, indicating that the two colors of the two kinds of color on the subject did not have a significant difference. The significance of the contrast between the visual gaze point indicators of the first and third categories of colors indicates that there is a significant difference between the two colors for the subjects The significance of the contrast between the second and third categories of color indicators P=0.166>0.05 indicates that there is no significant difference. This can be further verified that the vividness of the color has a significant effect on the visual gaze point, and the stronger the contrast, the greater the effect on the gaze point.

Table 8. Comparison of observation point significant analysis group

Serial number		Mean difference	Standard error	significance	95% confidence interval	
					Lower limit	Upper limit
1	2	-2.415	1.436	0.264	-5.84	1.23
	3	-5.106*	1.436	0.001	-8.74	-1.59
2	1	2.416	1.436	0.264	-1.25	5.58
	3	-2.741	1.436	0.166	-6.36	0.78
3	1	5.106*	1.436	0.001	1.55	8.69
	2	2.741	1.436	0.166	-0.86	6.32

3.3.2. Comparative analysis of graphics and copywriting. In the analysis of color and background elements, the main method used is the analysis of the salience of the overall visual indicators of the image, while for the copy as well as the logo, there are obvious areas in the image copy, so the analysis is carried out by way of dividing a specific area, and the size of the layout area of the copy has been changed, in order to check the effect of the change of the area of the copy on the attraction degree of the subject. The statistics of the attention time and attention point of the graphic and copywriting elements are shown in Table 9. In the group of copy elements of images, the ornaments are presented through three different forms, firstly, the ornaments are presented separately without copy description secondly, the ornaments are illustrated with copy, and the copy area is smaller thirdly, the copy is illustrated separately and the area is larger. After the statistical analysis of the visual indicators, it can be seen that the attention time of the graphic presentation is more than the attention time of the copy, and the process of increasing the area of the copy, the attention time and the data of the attention point are significantly improved.

Table 9. Graphic and copywriting elements look at time and focus point statistics

	Average fixation(ms)	SD	Fixation count(n)	SD
Graphic performance	258	81.6	5.8	3.9
Copywriting 1	211	66.2	4.6	2.6
Copywriting 2	236	53.8	15.8	5.3

The results of the significance analysis of the difference between graphic and copywriting indicators are shown in Table 10. According to the results of the significance analysis, it can be seen that the F-value between graphic performance and copywriting interpretation on the time of attention is 3.845, with significance P=0.028, which is significant. The value between graphic and copywriting at the point of gaze is 65.3 with significance P=0.021>0.01, which is significant.

Table 10. The results of the difference between graphics and copywriting indicators

	Mean square	F value	Significance
Fixation time(ms)	4315.6	3.845	0.028
Fixation point(n)	746.2	65.3	0.021

After analyzing the significance of different visual metrics between the two types of texts, the F-value of gaze time was 5.127, with significance $p=0.036<0.05$, indicating a significant difference. The F-value for gaze point is 66.3, significance $p=0.001<0.01$, indicating significant difference. It can be concluded that the size of the unit copy area is a determining factor in the size of the copy to attract visual attention, increase the same number of words copy area area, the attention of the copy of the effect of a significant increase in the actual operation of the process should also be considered in the layout design. The results of the analysis of the significance of the differences in indicators between different texts are shown in Table 11.

Table 11. The difference between copywriters is characterized by significant analysis

	Mean square	F value	significance
Fixation time(ms)	3295.6	5.127	0.036
Fixation point(n)	942.6	66.3	0.001

3.3.3. Comparative analysis of different types of signs. The statistics of gaze time and gaze point of graphic signs and letter signs are shown in Table 12. It is found that the average attention time of 279ms and the average attention point of 5.3 for graphic logos are larger than that of 234ms and 4.3 for letter logos, indicating that graphic logos attract more attention. The relatively large variance in attention time indicates that the attention level of logos varies greatly across subjects, partly due to differences in brand awareness.

Table 12. Graphic marks and letter markers' gaze time and observation point statistics

	Average fixation(ms)	SD	Fixation count(n)	SD
Graphic mark	279	69.2	5.3	2.8
Letter mark	234	67.5	4.3	1.5

The results of the significance analysis of the difference in indicators between graphic signs and letter signs are shown in Table 13. According to the results of the significance analysis of the table, the F-value of the different gaze times of the graphic signs and letter signs is 5.749, with significance $P=0.034<0.05$, which means that the significance difference is obvious. Whereas, the F-value for the point of gaze is 3.748 with significance $P=0.063$ and the significant difference is not significant, which is related to the size of the area of the sign.

Table 13. The results of the distinction between graphic and alphabetic indicators

	Mean square	F value	significance
Fixation time(ms)	7631.6	5.749	0.034
Fixation point(n)	18.655	3.748	0.063

Through ANOVA, summarize the test results of the test results of the significance effect of the changes of various types of visual elements of the subjects' plane images on the indicators of the eye movement experimental data, and the test results of the significant difference of the changes of visual elements are shown in Table 14. It can be seen through the test results, the change of color elements has no significant effect on the average gaze time of the subjects, but there is a significant difference in the average gaze point, indicating that the change of color can produce corresponding changes in the content of the plane image performance and the gaze area. In terms of copy setting, firstly, the attention effect of physical display is better than that of copy description, and there is also a significant difference in the experimental index between the two. On the other hand, the change in the size of the copy area has a significant difference in the attention time, and the difference in the attention point is even more obvious, indicating that the increase of the copy area in the image can significantly improve the attention effect of the copy. In the comparison of the different logo types, graphic logos outperformed letter logos and had a significant difference in mean gaze time, but no significant effect on mean gaze point.

Table 14. The results of the significant difference in visual factors

	Significant difference	
Comparison of visual elements	Average time	Average fixation point
Color variation	NO	obvious
Physical performance and copywriting interpretation	YES	obvious
Document area size	YES	obvious
Graphic mark and letter mark	obvious	NO

3.3.4. Comparative Analysis of Subjects. In the experimental design stage, the subjects were divided into professional-related and non-professional-related categories, in order to examine the influence of a priori knowledge on the effect of image attention, so in the results of the experimental data of the factors for the two categories of subjects to carry out statistical and significance analyses of the experimental indexes respectively. In the overall test results, the color elements and background elements of the change in the indicators between the two types of subjects is not much difference, but in the logo and copy elements produce a more obvious difference, the following analysis is carried out separately. In the color element picture group, a one-way ANOVA was conducted with both professional and non-professional subject groups as independent variables, and the significance analysis of the subjects' indicators for the color elements is shown in Table 15. The F-value of gaze time for the color element group was 1.153, with significance P=0.315, indicating no significant difference. The F-value for gaze point was 2.547, significant P=0.112>0.05, indicating no significant difference.

Table 15. The index significance analysis of the subjects was determined by subjects

	Fixation time		Fixation point	
	F value	significance	F value	significance
Color elements	1.153	0.315	2.547	0.112

The statistics of the subjects' gaze time and gaze points on the elements of the copy and the logo are shown in Table 16. From the statistics of the table, it can be seen that the eye movement data indexes of graphic vs. copy and graphic logo vs. letter logo comparisons are more obvious in the difference between the two types of subjects. In the graphic performance the attention time and gaze point of professional subjects are 222 and 13 respectively, both are more than the attention time and gaze point of non-professional subjects 215 and 10.The corresponding copy interpretation shows the opposite result, the attention time of non-professional subjects for the copy is more than that of professional subjects, which is 241ms and 189ms respectively.In the experiments of different types of signs, the graphic signs are obviously more In the experiments of different types of signs, graphic signs are obviously more attractive to non-professional objects, with more attention time and attention points than professional objects, while the attention of letter signs is 236ms longer than that of non-professional objects, and 208ms longer, with not much difference in attention points.

Table 16. The subject of the subject is measured by the time and the observation point

	Professional subjects		Non-professional subjects	
	Average	Average fixation	Average	Average fixation

	fixation(ms)	point(n)	fixation(ms)	point(n)
Graphic performance	222	13	215	10
Copy interpretation	189	9	241	9
Graphic mark	264	2	255	6
Letter mark	236	8	208	6

By conducting one-way ANOVA with two different types of subjects as independent variables for graphic and copywriting performance as well as gaze time and gaze point of graphic and letter logos, the significance analysis of the subjects' indicators for the elements of copywriting and logos is shown in Table 17. From the results of the significance analysis, it can be seen that under the conditions of the two elements of graphic performance and copywriting interpretation, the significance P of the gaze time of professional and non-professional subjects is 0.042 and 0.015, respectively, which is less than the significance level of 0.05, which indicates that there is a significant difference between the two types of subjects. On the graphic sign element, the significance P=0.426>0.05 for professional and non-professional subjects is not significant. Whereas, on letter sign elements soil, the significance P=0.036<0.05 for attention time of both types of subjects is significant.

Table 17. The index significance analysis of the elements was analyzed

	Fixation time		Fixation point	
	F value	significance	F value	significance
Graphic performance	0.784	0.042	0.066	0.812
Copy interpretation	0.145	0.015	3.512	0.031
Graphic mark	0.612	0.426	2.981	0.095
Letter mark	5.612	0.036	3.941	0.062

4. Conclusion

Based on the theory of computer-aided color design, this paper studies the color matching algorithm and the graphic layout generation method based on visual saliency in the computer-aided system. Through experimental tests, the corresponding conclusions are drawn as follows:

Comparing the automatic layout algorithms of MM'12 and IUI'12, the results of the systematic graphic layout realized by the method of this paper can achieve better appreciation.

Based on the research of image color selection, based on Monsignor Spencer's color reconciliation theory, the beauty of image color matching is quantified by introducing junction edge weights and correcting order factor values. The results show that the introduction of junction edge weights has a certain degree of rationality. The Pearson's correlation coefficients before and after the introduction of junction edge weights are 0.095 (p=0.781) and 0.315 (p=0.388), respectively, where the p-values are greater than 0.05.

References

[1] Ma, Q., & Lyu, P. (2021, August). Research on the application of computer-aided analysis system in the concept of visual aesthetics in graphic design. In Journal of Physics: Conference Series (Vol. 1992, No. 2, p. 022018). IOP Publishing.

[2] Zhao, C. (2021, March). A computer aided creative design method for cultural products. In 2021 International Conference on Intelligent Transportation, Big Data & Smart City (ICITBS) (pp. 346-349). IEEE.

[3] Wang, R. (2021). Computer-aided interaction of visual communication technology and art in new media scenes. Computer-Aided Design and Applications, 19(S3), 75-84.

[4] Wang, Z. (2023, February). Influence of Computer Aided Design Technology on Artistic Design Innovation. In 2023 IEEE International Conference on Integrated Circuits and Communication Systems (ICICACS) (pp. 1-5). IEEE.

[5] Hua, L., & Bowen, P. (2021, January). Analysis of ceramic design aesthetics under computer aided design. In 2021 2nd International Conference on Education, Knowledge and Information Management (ICEKIM) (pp. 770-773). IEEE.

[6] Adiji, B. E., & Ibiwoye, T. I. (2017). Effects of graphics and computer aided design software on the production of embroidered clothing in south Western Nigeria. Art and Design Review, 5(4), 230-240.

[7] Cui, H. (2024). Computer-aided design of hand-drawn art food packaging design based on a deep neural network model. International Journal for Simulation and Multidisciplinary Design Optimization, 15, 10.

[8] Liu, L., & Liu, G. (2022). Intelligent teaching method of interdisciplinary art design and CAD. Computer-Aided Design and Applications, 19(S8), 96-104.

[9] Xiao, Y. (2021). Research on visual image texture rendering for artistic aided design. Scientific Programming, 2021(1), 1190912.

[10] Yang, Y., & Ren, H. (2022). The teaching method combining art design and CAD design. Computer-Aided Design and Applications, 19(S8), 157-167.

[11] Xu, X., & Zheng, J. (2022). Evaluation of cultural creative product design based on computer-aided perceptual imagery system. Computer-Aided Design & Applications, 19(S3), 142-152.

[12] Zhang, Y. (2020). Computer-assisted human-computer interaction in visual communication. Computer-Aided Design and Applications, 18(1), 109-119.

[13] Hu, X. (2017). Research on the application of computer-aided art image generation based fractal method [J]. Revista de la Facultad de Ingenieria, 32(3), 1-9.

[14] Wu, X., & Yang, F. (2021, July). A study on the development of computer-aided design in the context of artificial intelligence. In Journal of Physics: Conference Series (Vol. 1982, No. 1, p. 012033). IOP Publishing.

[15] Zheng, R., & An, S. (2023). Digital art design and media practice integrating CAD and virtual reality technology. Computer-Aided Design and Applications, 20(S13), 86-97.

[16] Jamil, Z., & Ijaz, M. (2024). Abstract Art as an Inspiration to Create Textile Patterns through Computer Aided Designing. Proceedings of the Pakistan Academy of Sciences: A. Physical and Computational Sciences, 61(2), 203-216.

[17] Tsai,Hung & Hung. (2007). Computer Aided Product Color Design with Artificial Intelligence. Computer-Aided Design and Applications(1-4),557-564.

[18] Giovanni Moretti,Stephen Marsland & Paul Lyons. (2013). Computational production of colour harmony. Part 2: Experimental evaluation of a tool for gui colour scheme creation. Color Research & Application(3),218-228.

[19] Wenshuo Zhu,Yuan Xue,Yourong Chen,Yaojun Wang & Huanqiang Shi. (2023). Construction of grid color mixture model of seven primary-color and modified Stearns-Noechel color matching algorithm for color prediction of full-color-gamut rotor melange yarn. Journal of Engineered Fibers and Fabrics.

[20] Deng Li,Zhou Fangyuan & Zhang Zhirui. (2022). Interactive genetic color matching design of cultural and creative products considering color image and visual aesthetics. Heliyon(9),e10768-e10768.